

# Pulsar acceleration by asymmetric emission of sterile neutrinos

Enrico Nardi<sup>1</sup>

*Theory Division, CERN CH-1211 Geneva 23, Switzerland*

enardi@naima.udea.edu.co

and

Jorge I. Zuluaga

*Departamento de Física, Universidad de Antioquia, A.A. 1226, Medellín, Colombia*

jzuluaga@naima.udea.edu.co

## ABSTRACT

A convincing explanation for the observed pulsar large peculiar velocities is still missing. We argue that any viable particle physics solution would most likely involve the resonant production of a non-interacting neutrino  $\nu_s$  of mass  $m_{\nu_s} \sim 20\text{--}50$  keV. We propose a model where anisotropic magnetic field configurations strongly bias the resonant spin flavour precession of tau antineutrinos into  $\nu_s$ . For internal magnetic fields  $B_{\text{int}} \gtrsim 10^{15}$  G a  $\bar{\nu}_\tau\text{--}\nu_s$  transition magnetic moment of the order of  $10^{-12}$  Bohr magnetons is required. The asymmetric emission of  $\nu_s$  from the core can produce sizeable natal kicks and account for recoil velocities of several hundred kilometers per second.

*Subject headings:* elementary particles — pulsars: general — stars: neutron — supernovae: general

## 1. INTRODUCTION

Measurements of the pulsars proper motion have shown that the pulsar population is characterized by peculiar velocities much higher than those of all other stellar populations (Gunn & Ostriker 1970; Lyne & Lorimer 1994; Hansen & Phinney 1997; Cordes & Chernoff 1997; Lorimer, Bailes, & Harrison 1997). While the precise form of the velocity distribution is uncertain, recent studies indicate that it must extend to  $\sim 1000$  km  $\text{s}^{-1}$ , with a mean of  $\sim 500$  km  $\text{s}^{-1}$  (Lorimer et al. 1997). Since the velocities of pulsars' likely progenitors, the massive stars, are among the lowest in the galaxy ( $\sim 10\text{--}40$  km  $\text{s}^{-1}$ ) it is natural to think that the mechanism responsible for their acceleration can be related either to supernova (SN) core collapse and explosion, or to the post-explosion cooling phase when, within a few

seconds, a huge amount of energy is emitted from the proto-neutron star (PNS) through the radiation of  $\sim 10^{58}$  neutrinos of all flavours.

To date, no convincing physical process that could account for pulsar acceleration has been identified (a review of different kick mechanisms has been recently given by Lai (1999)). The astrophysical solutions that have been proposed include, in broad terms, the possibility of symmetric and of asymmetric SN explosions. In the first case, large recoil velocities are achieved in response to the mass loss in the (symmetric) explosion of one component of a close binary system (Gott, Gunn, & Ostriker 1970; Iben & Tutukov 1996, 1997). It was shown that the remnant can achieve velocities comparable to the orbital velocity of the SN progenitor. However, detailed Monte Carlo simulations of binaries' evolution through the SN phase fail to reproduce the observed velocity distributions of pulsars and hint at asymmetric explosions (Lorimer et al. 1997; Dewey & Cordes 1987;

<sup>1</sup>Permanent address: Departamento de Física, Universidad de Antioquia, A.A. 1226, Medellín, Colombia

van den Heuvel & van Paradijs 1997; Hughes & Bailes 1999). In the second case, asymmetrical stellar collapse and explosion occurs because of pre-explosion instabilities and core density distortions, imparting to the residue an intrinsic kick (Janka & Mueller 1994; Burrows & Hayes 1995, 1996). The momentum scale of the mass ejecta in the SN explosion is of the order of  $\approx 6 \times 10^{53}$  erg/c, corresponding to about ten solar masses ejected with velocities  $\approx 10^4$  km s<sup>-1</sup>. Then, to accelerate the remnant of about  $1.5 M_{\odot}$  to the largest observed velocities, it is necessary to generate a momentum asymmetry in the ejecta of the order of a few per cent. The asymmetric explosion scenario remains unsatisfactory in the sense that initial anisotropies in the collapsing core sufficiently large to generate asymmetries of this size have to be input artificially (Burrows & Hayes 1996) and, from the point of view of present (2-D) hydrodynamic calculations, are difficult to justify (Janka & Mueller 1994).

More recently it has been suggested that a completely different class of mechanisms could be responsible for imparting a natal kick to the neutron star. Virtually all the gravitational binding energy released during the collapse of the progenitor iron core ( $\approx 3 \times 10^{53}$  ergs) is emitted during the first 10 seconds after core bounce in the form of neutrinos and antineutrinos. The momentum in neutrinos is therefore comparable to the momentum in the ejected matter. Hence, also in this case a few per cent asymmetry in the neutrino emission could suffice to account for the largest velocities observed. The particle physics explanations for the pulsar acceleration mechanisms can be classified according to the underlying mechanism at the origin of the momentum asymmetry in the neutrino emission. The asymmetry could be in the *number* of neutrinos, or in the neutrino *energy* (since the number of neutrinos is not conserved when neutrinos stream out of the core, this only refers to the microscopic cause of the asymmetry, and does not describe the macroscopic effect). In both cases, the presence of a strong magnetic field  $B \sim 10^{15}$ – $10^{16}$  G provides the asymmetric initial condition for the system. In the first case, parity violation in electroweak interactions was thought to be at the origin of asymmetric neutrino emission from strongly magnetized PNS. The cumulative effect of multiple neutrino scat-

terings off the slightly polarized nucleons would result in a sizeable anisotropy in the neutrino momentum (Horowitz & Piekarewicz 1998; Horowitz & Li 1998; Lai & Quian 1998a). More detailed studies showed that this effect was largely overestimated (Kusenko, Segré, & Vilenkin 1998; Arras & Lai 1999). When neutrinos are in local thermodynamic equilibrium (as they are to a very good approximation in the interior of a PNS) detailed balance ensures that no cumulative effect from multiple scatterings can build up. Local effects in the PNS atmosphere, as for example the deviations from thermal equilibrium that occur close to the neutrinosphere, can generate asymmetries in the neutrino emission. However, to date detailed analyses of these effects have failed to produce kicks as large as  $1000$  km s<sup>-1</sup> (Arras & Lai 1999). The second case relies on the assumption that resonant transitions (oscillations (Kusenko & Segré 1996, 1997; Grasso, Nunokawa, & Valle 1998) or spin-flavour precession (Akhmedov, Lanza, & Sciama 1997)) between different neutrino flavours occur inside the PNS. The resonance surface for the conversion becomes the effective surface of last scattering (the neutrinosphere) for the neutrino flavour with the largest mean free path. Since a strong magnetic field can slightly distort the resonance surface, neutrinos are emitted from regions with different temperatures, which yields an asymmetry in the overall momentum. Also in this case, the real effect was largely overestimated. This is because the variation of the temperature over the effective neutrinosphere cannot be directly related to an anisotropy in the neutrino energy. The energy flow from the star is governed by the inner core emission of neutrinos; in first approximation, local processes in the PNS atmosphere, where the resonant conversion takes place, cannot modify the (isotropic) neutrino emission from the core (Janka & Raffelt 1999).

In conclusion, both the macroscopic parity violation and the resonant neutrino conversion scenario, which for a while seemed to provide elegant particle physics mechanisms to account for pulsars' acceleration, did not survive more detailed analysis. However, the study of these attempts and of the reasons why they fail to produce natal kicks of the right magnitude can guide us to infer some of the conditions that must be satisfied by a viable particle physics solution.

- The neutrino observations from SN1987A, and in particular the duration of the  $\bar{\nu}_e$  burst, support the theoretical expectation that active neutrinos are copiously produced inside the PNS core and that they are the main agents of the energy emission. Theoretical studies indicate that, to a good approximation, the total energy carried away by neutrinos is equipartitioned among the six neutrino and antineutrino flavours (Janka 1995). This implies that conversions between the active flavours would simply result in exchanging the respective spectra, and cannot affect the main characteristics of energy emission (Janka & Raffelt 1999). We learn from this that if neutrino conversion is responsible for the kicks, then the conversion must be into some new particle that does not interact with matter in the same way than the standard neutrinos: most probably a very weakly interacting or sterile neutrino  $\nu_s$ .
- In thermal equilibrium, the microscopic peculiarities of neutrino scattering processes cannot build up any macroscopic asymmetry. This applies also to possible neutrino scattering into new exotic states. This hints at some macroscopic condition anisotropically realized inside the PNS. If this has to influence the neutrino conversion rates, we are naturally led to thinking at some asymmetrically located resonance, or at local violation of the adiabaticity conditions for the conversion.
- An anisotropic resonant conversion of an active neutrino into an exotic state is still not sufficient to generate a momentum asymmetry. Close to the resonance region the parent  $\nu$  and the  $\nu_s$  would both have an asymmetric momentum distribution, but their asymmetries would compensate in the total momentum. However, a non-interacting  $\nu_s$  would freely escape from the PNS, thus preserving its original asymmetry, while the active neutrino keeps interacting with the background particles. If  $\nu$  has enough time to recover a symmetric momentum distribution before escaping from the star, then the  $\nu_s$  asymmetry will be left unbalanced. This suggests

that the conversion should occur far inside the  $\nu$  neutrinosphere, and most likely in the high-density regions close to the core.

The picture emerging from these considerations is a resonant conversion of an active flavour into a non-interacting neutrino, at the large densities and temperatures typical of the PNS regions close to the core. In turn, matching the resonance condition hints at a sterile neutrino mass  $\approx 20\text{--}50$  keV. In order to implement the previous scheme it is important to identify all the possible macroscopic asymmetries of the system. As we will discuss in the next section, there are observational indications that, in some cases, pulsar magnetic fields are better described by an off-centred dipole, rather than simply by an oblique dipole with the centre of the magnetic axis coinciding with the centre of the star. Clearly this implies anisotropic conditions inside the PNS core, since the magnetic field strength can easily vary by more than one order of magnitude within regions of equal matter density. Then it is not difficult to envisage how in such an anisotropic background the Mikheyev–Smirnov–Wolfenstein (MSW) mechanism for matter-enhanced neutrino oscillations (Wolfenstein 1978; Mikheev & Smirnov 1985) or resonant spin-flavour precession (RSFP) (Akhmedov 1988a, 1988b; Lim & Marciano 1988) could result in large asymmetries in the rate of neutrino conversion between opposite hemispheres. Moreover, if the conversion involves non-interacting neutrinos, they will freely escape from the core, yielding a large momentum asymmetry. We stress that the solution we are proposing here is intrinsically different from previously studied mechanisms that exploit resonant neutrino conversion and emission from a slightly deformed resonance surface (Kusenko & Segré 1996, 1997; Grasso et al. 1998; Akhmedov et al. 1997). In our case, it is the conversion probability that is not isotropically distributed inside the (spherical) region where the resonant condition is satisfied.

In Section 2 we will review some of the arguments in support of our basic assumption that the magnetic field in the PNS interior can be characterized by sizeable anisotropies. In Section 3 we will briefly review the physics of RSFP. For definiteness, we will assume that tau antineutrinos can be resonantly converted into sterile neutrinos  $\nu_s$ .

We will show that for acceptable values of the PNS magnetic field and of the neutrino transition magnetic moment  $\mu_\nu$  the adiabaticity conditions for an efficient conversion are satisfied in regions asymmetrically displaced from the star centre. A MSW solution to the problem can also be implemented straightforwardly, since the asymmetrically polarized background results in an anisotropic neutrino potential (Nunokawa et al. 1997). However, this requires more fine tuning in the choice of the relevant parameters and we will only comment briefly on this possibility. The details of the PNS model we have used and of neutrino diffusion from the core will be described in Section 4. Finally in Section 5 we will present our results and draw the conclusions.

## 2. EVIDENCE FOR ANISOTROPIC MAGNETIC FIELDS

The evidence in support of asymmetric magnetic field topologies for variable magnetic stars and pulsars was discussed long ago by Harrison and Tademaru (Harrison & Tademaru 1975; Tademaru & Harrison 1975; Tademaru 1976). They argued that pulsars' magnetic fields can be well modeled by an off-centred magnetic dipole, displaced from the centre of the star and oriented obliquely with respect to the rotation axis in an arbitrary direction. They also showed that such a field configuration radiates asymmetrically low-frequency electromagnetic radiation, and they tried to explain through this mechanism 'post-natal' pulsar acceleration at the expense of the star rotational energy. However, velocities much in excess of  $100 \text{ km s}^{-1}$  cannot be explained in this way, since for typical rotational periods of the order of 10 ms the rotational energy does not exceed by much the total kinetic energy of the star. Moreover, the lack of any observed correlation between the magnetic field and the transverse velocity, or between the direction of the motion and the magnetic axis (Lorimer et al. 1997; Deshpande, Ramachandra, & Radhakrishnan 1999) has virtually ruled out the post-natal acceleration model. Asymmetric magnetic field configurations can also affect  $\nu_e$  and  $\bar{\nu}_e$  absorption cross sections on neutrons and protons. Lai and Qian (1998b) studied the possible asymmetry in the neutrino emission that can be generated in this way, and showed that the effect is again too small to produce appreciable kicks.

However, an anisotropic magnetic field can still be responsible for pulsar acceleration by producing sizeable asymmetries in the neutrino emission during the early PNS cooling phase. In principle, the mechanism we want to propose can be effective independent of the particular type of magnetic field model, as long as it predicts sizeable anisotropies in the field strength. However, for definiteness we will concentrate on the simple off-centred and decentred magnetic dipole models (Harrison & Tademaru 1975; Tademaru & Harrison 1975; Tademaru 1976) also because they are supported by a few observational evidences. Decentred dipole models were first introduced in the attempt to improve the representation of the fields of periodic magnetic variable stars (Landstreet 1970). It was later suggested that these models could also account for special features in the electromagnetic emission of the so-called interpulse pulsars, which are characterized by secondary interulses well separated from the main pulse, and of an intensity up to two orders of magnitude smaller (Hankins 1986). A displacement of the magnetic dipole along the magnetic axis of an amount  $\delta$  in units of stellar radius would produce unequal surface field intensities in the ratio  $(1 + \delta)^3 / (1 - \delta)^3$ , providing a simple explanation for the relative weakness of the secondary interpulse. The decentre parameter  $\delta$  inferred from observational studies of variable magnetic stars and interpulse pulsars ranges between 0.1 and 0.6 (Harrison & Tademaru 1975; Tademaru & Harrison 1975; Tademaru 1976). In some cases surface fields of opposite polarities, separated by much less than  $180^\circ$  have been observed (Hankins 1986). Asymmetries of this kind are not explained by the simple decentred model, and suggest that the dipole is actually *off-centred*. Namely, the magnetic dipole  $\mu = (\mu_z, \mu_\rho, \mu_\phi)$  (in cylindrical coordinates) is arbitrarily oriented and displaced from the centre of the star by an amount  $\delta_z$  along the spin axis and  $\delta_\rho$  in the radial direction. Since the dipole axis does not intersect the spin axis, the angular separation between the main and the secondary pulses is easily accounted for.

The study of interpulse pulsars is statistically limited by the small sample of a few per cent of all pulsar population. This is likely to be due to the fact that both the angle of inclination between the rotation axis and the line of sight, and the angle between the spin and the magnetic axis, must

be close to  $90^\circ$  to allow for their detection. Still, the few direct observations available today suggest that it is not unreasonable to assume that most pulsars have oblique and off-centred dipole fields, or possibly some more complicated field configuration implying sizeable anisotropies in the magnetic field topology.

Since off-centred dipoles radiate energy at a different rate with respect to centred dipoles, one might wonder if off-centred models could be tested by measuring the pulsar rate of energy loss. In simple cases, the loss of angular velocity  $\dot{\omega}$  of a pulsar can be described by the law

$$\dot{\omega} = -k\omega^n, \quad (1)$$

where  $n$ , called the *braking index*, can be directly inferred from the instantaneous rate of change of frequency through the relation  $n = \ddot{\omega}\omega/\dot{\omega}^2$ . A magnetic dipole  $\mu$  located on the spin axis radiates electromagnetic energy at the expense of rotational energy at a rate

$$\frac{dE_\mu}{dt} = -\frac{1}{2} \frac{d(I\omega^2)}{dt} = \frac{2\mu_\rho^2}{3c^3} \omega^4, \quad (2)$$

where  $I$  is the neutron star moment of inertia. For constant  $I$  this yields  $n = 3$ . For gravitational quadrupole radiation, denoting by  $M_\rho$  the component of the mass-quadrupole orthogonal to the spin axis,  $dE_M/dt = (G_N M_\rho^2/45c^5) \omega^6$  is found (Ostriker & Gunn 1969), and the braking index is  $n = 5$ . For a magnetic dipole displaced from the spin axis by an amount  $\delta_\rho R$ , the spin-down law reads

$$\dot{\omega} = -k\omega^3 (1 + \alpha\omega^2) \quad (3)$$

where  $k = 2\mu_\rho^2/3Ic^3$  and  $\alpha = 2\mu_z^2(\delta_\rho R)^2/5\mu_\rho^2 c^2$ . This yields a braking index  $n = \ddot{\omega}\omega/\dot{\omega}^2 \simeq 3 + 2\alpha\omega^2 > 3$ . Unfortunately, for typical values of the relevant parameters ( $P \sim 10$  ms,  $R \sim 10$  km, etc.) one obtains  $\alpha\omega^2 \lesssim 10^{-5}$ , and thus the deviation from the centred dipole spin-down law is by far too small to be measurable.

### 3. RESONANT SPIN-FLAVOUR PRECESSION

The mechanism we want to explore to account for pulsar acceleration is the RSFP of an active neutrino into a sterile neutrino, driven by the anisotropic magnetic field of a decentred dipole

configuration. For simplicity, we will not analyze here the more realistic case of an off-centred magnetic dipole or of more complicated configurations, since these generalizations do not change our main results. We just note that, in the off-centred case, sterile neutrino emission could contribute not only to the acceleration, but also to a spin-up of the PNS. As has recently been suggested (Spruit & Phinney 1998) the rotating core of the pulsar progenitor might have just a tiny fraction of the angular momentum required to explain the observed rotation velocities of pulsars. For this reason it was conjectured that the same physical process that kicks the PNS at birth could be responsible also for pulsars' fast rotations (Spruit & Phinney 1998; Cowsik 1998). Thus, it might be interesting to study if a more general magnetic field configuration, in conjunction with neutrino RSFP, could also account for the observed pulsars periods.

We start by assuming that  $\bar{\nu}_\tau \rightarrow \nu_s$  RSFP can occur at neutron star core densities and magnetic field strengths. Since  $\nu_s$  can freely escape from the core, we need to ensure that the neutrino burst duration  $\sim 10$  s will not be shortened too much. Assuming equal luminosity for all neutrino and antineutrino flavours (Janka 1995), even a 100% efficient conversion of  $\bar{\nu}_\tau$  into  $\nu_s$  would affect only  $1/6 \sim 17\%$  of the energy in the game. Since there are resonance regions where the adiabaticity conditions are not satisfied and no conversion occurs, the overall efficiency for  $\bar{\nu}_\tau \rightarrow \nu_s$  conversion is in fact lower, meaning that the amount of energy carried away by  $\nu_s$  is small enough for the burst duration not to be drastically changed. On the other hand a 10%–20% asymmetry in the active–sterile conversion efficiency between opposite hemispheres would result in a few per cent asymmetry in the total momentum, as is needed to explain the largest velocities observed. An important point in this discussion is to ensure that transitions that involve other active flavours, such as  $\bar{\nu}_{e,\mu} \rightarrow \bar{\nu}_\tau \rightarrow \nu_s$ , will not result in an energy ‘siphon’ effect that would cool the PNS too rapidly. Indeed, in the light of the present experimental hints for non-vanishing neutrino mixings, accounting for these reactions is mandatory. The rates for neutrino flavour conversion in a neutron star core were studied by Raffelt and Sigl (1997) and by Hannestad et al. (1999). For  $\nu_e$  the large charged current (CC) refractive effects

due to the background electrons strongly suppress any in-matter mixing angle, so that conversion to other neutrino species cannot occur on the time scale of neutrino diffusion (Raffelt & Sigl 1993). Also for  $\nu_\mu \leftrightarrow \nu_\tau$  the conversion time scale safely exceeds the neutrino diffusion time (Hannestad et al. 1999). This is due to the presence of a small amount of muons in the hot superdense core, which implies additional CC contributions to the  $\nu_\mu$  index of refraction, as well as to the second-order difference in the  $\nu_\mu$ - $\nu_\tau$  neutral current (NC) potentials  $\delta V \sim G_F^2 m_\tau^2 N_N$  (where  $N_N$  is the density of nucleons) (Botella, Lim, & Marciano 1987). In conclusion, the large differences in the neutrinos indices of refraction inside the PNS guarantee that  $e$ ,  $\mu$  and  $\tau$  lepton numbers are separately conserved, and thus the conversion into  $\nu_s$  will affect just one neutrino flavour.

The condition for a RSFP of  $\bar{\nu}_\tau$  into sterile neutrinos  $\nu_s$  reads

$$V(\bar{\nu}_\tau) = \frac{G_F N_n}{\sqrt{2}} - \sum_{f=n,p,e} \kappa_f \langle \lambda_{\parallel}^f \rangle = \frac{\Delta m^2}{2E}. \quad (4)$$

The effective potential  $V(\bar{\nu}_\tau)$  felt by a  $\bar{\nu}_\tau$  propagating in the hot, superdense and slightly polarized PNS matter has two contributions: the first one is due to the coherent vector interaction with the background and is proportional to the number density of neutrons  $N_n$ . The second one, which is due to coherent axial-vector interactions, is proportional to the average polarization  $\langle \lambda_{\parallel}^f \rangle$  of the  $f = n, p, e$  background fermion parallel to the direction of the neutrino motion (Nunokawa et al. 1997; Bergmann, Grossman, & Nardi 1999). The proportionality factor  $k_f \sim (g_A^f G_F / \sqrt{2}) N_f$  depends on the  $f$ -fermion number density  $N_f$  and on its axial-vector coupling  $g_A^f$ . In the right-hand side of equation (4),  $\Delta m^2$  denotes the square mass difference between the tau and the sterile neutrino masses. In the PNS core  $V(\bar{\nu}_\tau) \approx 4 \times 10^{-6} \rho_{14} \text{ MeV}$ , where  $\rho_{14} = \rho / 10^{14} \text{ g cm}^{-3}$ . For neutrino thermal energies of the order  $E_\nu \sim 100\text{--}200 \text{ MeV}$  the resonance condition can be satisfied if  $\Delta m^2 \sim (20\text{--}50 \text{ keV})^2$ . This value is much larger than the cosmological limit  $m_{\nu_\tau}$  ( $\lesssim 10^2 \text{ eV}$ ), and in the following we will therefore assume  $\Delta m^2 = m_{\nu_s}^2 - m_{\nu_\tau}^2 \simeq m_{\nu_s}^2$ .

The average background polarization contributing to the second term in  $V(\bar{\nu}_\tau)$  grows lin-

early with the magnetic field, which in a neutron star can reach extremely high values, up to  $\sim 10^{15} \text{ G}$  (Thomson & Duncan 1992, 1993, 1995, 1996). However, during the early cooling phase when most of the neutrinos are emitted, the temperature is also large, the electrons are relativistic and degenerate, and as a result the induced polarizations are strongly suppressed, down to  $\langle \lambda_{n,p} \rangle \lesssim 10^{-3} \times B_{15}$  and  $\langle \lambda_e \rangle \lesssim 10^{-2} \times B_{15}$  (Bergmann et al. 1999), where  $B_{15}$  is the magnetic field strength in units of  $10^{15} \text{ G}$ . Thus in general  $\kappa_f \langle \lambda_{\parallel}^f \rangle \ll G_F N_n / \sqrt{2}$  and, in most cases, neglecting the polarization term is well justified.

The resonance condition for the (helicity-conserving) MSW effect ( $\bar{\nu}_\tau \leftrightarrow \bar{\nu}_s$ ) has the same form that equation (4) except for the fact that the right-hand side is multiplied by  $\cos 2\theta_V$ , where  $\theta_V$  is the vacuum mixing angle. Because the magnetic dipole configuration is asymmetric, in different regions of a core shell of given neutron density  $N_n$  the magnetic field and the average polarization  $\langle \lambda^f \rangle$  can be vastly different. Then it could be possible that the resonance condition is satisfied with sufficient accuracy in just one hemisphere. This can be more easily achieved for resonant  $\bar{\nu}_e \leftrightarrow \bar{\nu}_s$  oscillations, since in this case the neutron number density in the first term in equation (4) is replaced by  $N_n - 2N_e$ , and in some region of the core and at some stage of the PNS evolution this combination can approach values close to zero. However, local violation of the adiabaticity condition for a RSFP conversion (see below) appears to be more natural than an asymmetric MSW resonant conversion, in the sense that it can be satisfied for a larger range of the relevant parameters, and is also more stable with respect to core evolution during the deleptonization and cooling phases. Therefore in the following we will concentrate on the RSFP conversion mechanism.

Once the condition in equation (4) is satisfied, the probability  $P_{\bar{\nu}_\tau \leftrightarrow \nu_s}$  that a spin-flavour neutrino transition will occur depends on its degree of adiabaticity. To a good accuracy

$$P_{\bar{\nu}_\tau \leftrightarrow \nu_s} \simeq 1 - \exp\left(-\frac{\pi}{2} \gamma\right), \quad (5)$$

which is sizeable when  $\gamma \gtrsim 1$ . Denoting by  $\ell_\rho \equiv |(1/\rho)(d\rho/dr)|^{-1}$  the characteristic length over which the density varies significantly, and with  $\ell_{\rho \text{ res}}$  its value at the resonance, the adia-

baticity parameter  $\gamma$  can be written as (Akhmedov 1997; Akhmedov et al. 1997)

$$\gamma \simeq 1.04 \left( \frac{1}{1 - Y_e} \right) \left( \frac{2.6 \times 10^{14} \text{ g cm}^{-3}}{\rho} \right) \times \left( \frac{\mu_\nu}{10^{-12} \mu_B} \frac{B_{\perp \text{res}}}{3 \times 10^{15} \text{ G}} \right)^2 \frac{\ell_{\rho \text{res}}}{10 \text{ km}}, \quad (6)$$

where  $Y_e \approx 0.3$  is the number of electrons per baryon in the PNS core (Burrows & Lattimer 1986),  $\mu_B$  is the Bohr magneton and  $B_{\perp}^{\text{res}}$  is the value at resonance of the magnetic field component orthogonal to the direction of neutrino propagation. Let us now assume that the magnetic dipole is displaced from the star centre by an amount  $\delta$  in units of the PNS radius  $R$ , and let us define  $\hat{\delta} = \delta \cdot (R/R_{\text{res}})$ , where  $R_{\text{res}}$  is the location of the resonance layer. For reasonable values  $\hat{\delta} \approx 0.2$ – $0.5$  the ratio of field intensities between the north (N) and south (S) magnetic poles of the resonance shell  $B_S^{\text{res}}/B_N^{\text{res}} \simeq (1 - \hat{\delta})^3 / (1 + \hat{\delta})^3$  falls in the range  $10^{-1}$ – $10^{-2}$ . Then from equation (6) we see that the condition  $\gamma_N \gtrsim 1$  ( $P_{\bar{\nu}_\tau \leftrightarrow \nu_s} \sim 1$ ) and  $\gamma_S \ll 1$  ( $P_{\bar{\nu}_\tau \leftrightarrow \nu_s} \sim 0$ ) that triggers the anisotropic neutrino emission can be realized in a natural way. In Fig. 1 we depict the variation of the adiabaticity parameter  $\gamma$  inside the resonance layer as a function of the angular distance  $\Theta$  from the magnetic dipole axis. The resonance is located at  $R_{\text{res}} = 1.5 R_c$ , where  $R_c$  denotes the core radius, and the maximum value of the magnetic field strength at resonance is  $B = 4 \times 10^{15} \text{ G}$ . For small values of the decentred parameter  $\delta \sim 0.1$  the adiabaticity condition is matched in both hemispheres and no large asymmetry can be expected. However, for  $\delta > 0.2$  we get  $\gamma < 1$  in the whole hemisphere  $\Theta > \pi/2$  and a sizeable asymmetry can be produced. It is also apparent that if  $\delta$  becomes too large, the region where the adiabaticity condition is satisfied shrinks down to a small cone (e.g. for  $\delta \gtrsim 0.5$  there is good adiabaticity only when  $\Theta \lesssim \pi/6$ ). This heavily reduces the conversion efficiency and results in a suppression of the asymmetry. It also suggests that no simple correlation between the value of  $\delta$  and the overall  $\nu_s$  momentum asymmetry can be expected.

Let us now comment briefly on the possible values of the relevant physical quantities appearing in equation (6). Magnetic field strengths  $\gtrsim 10^{15} \text{ G}$  are not unreasonable in the interior of

a new-born neutron star. Indeed, there is observational evidence for highly magnetized young pulsars (magnetars) with dipole *surface* fields as large as  $8 \times 10^{14} \text{ G}$  (Hurley 1999). On the other hand, theoretical studies indicate that internal dipole fields as large as  $B_{\text{int}} \sim (5\text{--}10) \times 10^{15} \text{ G}$  can be formed during the first few seconds after gravitational collapse, when the strong convective motions coupled with rapid rotation can produce an efficient dynamo action (Thomson & Duncan 1992, 1993, 1995, 1996). As regards the value of  $\mu_\nu$ , it is well known that the RSFP conversion mechanism requires rather large transition magnetic moments. For densities close to nuclear density ( $\approx 2.6 \times \rho_{14}$ ) and acceptable values of the magnetic field, the adiabaticity condition in equation (6) points towards magnetic moments of the order of  $10^{-12} \mu_B$ . For  $\bar{\nu}_\tau$  this is several orders of magnitude below the laboratory limits (Groom et al. 1998). In the early Universe,  $\nu_s$  will attain thermal equilibrium only for  $\mu_\nu \gtrsim 6 \times 10^{-11} \mu_B$  (Elmfors et al. 1997) and hence the nucleosynthesis constraints can be easily satisfied. The astrophysical limit  $\mu_\nu \lesssim 3 \times 10^{-12} \mu_B$  implied by stellar energy-loss arguments (Raffelt 1990) does not apply in this case, since the final-state sterile neutrino with  $m_s \gg 5 \text{ keV}$  is too heavy to be produced inside red-giants or white-dwarfs. Assuming, as is reasonable, that the main  $\nu_s$  decay mode is radiative  $\nu_s \rightarrow \bar{\nu}_\tau \gamma$ , the limits on  $\gamma$ -ray fluence immediately after the arrival of the neutrino burst from the SN1987A can be used to set strong constraints on  $\mu_\nu$ . Under the assumption that the decaying neutrinos are carrying away about 1/3 of the total energy, the limit  $\mu_\nu < 1.6 \times 10^{-14} \mu_B$  (10 keV/ $m_{\nu_s}$ ) was derived (Oberauer et al. 1993; Raffelt 1996, p.474). However, this limit cannot be straightforwardly applied to our case. As we will see below, depending on the overall conversion efficiency, the  $\nu_s$  can easily carry an overall energy more than one order of magnitude smaller than what was assumed in order to derive this limit. It is even conceivable that no conversion at all could have occurred for SN1987A, if the magnetic field was too weak to satisfy the adiabaticity condition (of course this would also imply no intrinsic kick for the SN1987A residue, which unfortunately has not been detected). In addition to this, in our framework the  $\nu_s$  emission is strongly anisotropic, and beaming effects could have drastically reduced the

flux along the line of sight of the Earth. We conclude that the SN1987A limit cannot exclude values of  $\mu_\nu$  of the order  $10^{-12}\mu_B$ . However, it is interesting to note that a clear signature of the mechanism we are proposing would be a large flux of  $\gamma$  rays with energies of several tens of MeV from the next galactic SN. Since the  $\nu_s$  are emitted from regions close to the hot inner core, this would also be accompanied by an anomalous spectral component of  $\bar{\nu}_\tau$  from  $\nu_s$  decays with a temperature about one order of magnitude larger than the  $\nu_\tau$  and  $\nu_\mu$  spectra.

If  $\mu_\nu \gtrsim \text{few} \times 10^{-12}\mu_B$  the sterile neutrinos would be directly produced through helicity flipping scattering off electrons and protons (Barbieri & Mohapatra 1989; Ayala, D’Olivo, & Torres 2000). The main concern here is not so much the change in the rate of energy loss, since this would affect only one flavour, but rather the fact that spin-flips due to scattering processes would then occur within the entire core volume with an (almost) isotropic distribution. If the time scale for these processes is much shorter than the  $\bar{\nu}_\tau$  diffusion time to the resonant region, almost all the  $\bar{\nu}_\tau$  will convert into  $\nu_s$  inside the core. However, in crossing the resonance layer, the  $\nu_s$  will be anisotropically reconverted into interacting states. This would result in approximately the same momentum asymmetry, but in the opposite direction. If the time scale for the helicity flipping scatterings is much larger than the  $\bar{\nu}_\tau$  diffusion time to the resonance (but of course shorter than their diffusion time to the neutrinosphere) the  $\nu_s$  asymmetry generated at the resonance surface will be preserved. This is because the unconverted  $\bar{\nu}_\tau$  streaming out from the resonance layer will quickly recover an isotropic momentum distribution, so that the later emission of  $\nu_s$  from helicity flipping scatterings will be essentially symmetrical. Still, allowing for these possibilities would unnecessarily complicate our analysis. Therefore, to ensure that helicity flipping scatterings are safely suppressed and will not interfere with resonant conversions, we will assume that the limit  $\mu_\nu \lesssim \text{few} \times 10^{-12}\mu_B$  (Barbieri & Mohapatra 1989; Ayala et al. 2000) is satisfied.

#### 4. THE PROTO-NEUTRON STAR MODEL

In this section we describe the model that was used to simulate the PNS physical conditions dur-

ing the first few seconds after core bounce. Our PNS model is three dimensional but static, so that the results we will obtain should be understood as a “proof-of-principle” calculation of the possible size of the momentum asymmetry. We identify four different regions that are of major importance for the conversion process and for the neutrino emission:

- 1) *Core–atmosphere interface* ( $r = R_c$ ). Neutrinos are mainly produced within the hot and dense core, where the density varies slowly with the radius. From the central regions with supernuclear density  $\rho_o \simeq 8 \times \rho_{14}$  the density decreases down to nuclear density  $\rho_c \simeq 2.6 \times \rho_{14}$ . We define the core–atmosphere interface radius  $R_c$  through  $\rho(R_c) = \rho_c$ , where  $R_c \approx 10$  km.
- 2) *Resonance layer* ( $r = R_{\text{res}}$ ). This is the region where the (energy-dependent) resonance condition in equation (4) is satisfied. When the adiabaticity condition  $\gamma \gtrsim 1$  is fulfilled, this is also the region of emission of the sterile neutrinos. In our simulation we have studied the range  $R_{\text{res}}/R_c = 0.8\text{--}1.8$ , namely we have assumed that the resonance layer is close to the core–atmosphere interface.
- 3) *Neutrino energy–sphere* ( $r = R_E$ ). The main reactions through which the  $\bar{\nu}_\tau$  exchange energy with the stellar gas are NC scattering off electrons and neutrino pair processes. The neutrino energy sphere is defined as the region where the  $\bar{\nu}_\tau$  undergo the last inelastic interaction with the background particles. For  $r > R_E$ , neutrinos mainly scatter off nucleons. While this determines the neutrino transport opacity, the amount of energy exchanged is negligible, so that outside the energy–sphere the neutrinos start being thermally disconnected from the medium.
- 4) *Neutrino transport–sphere (neutrinosphere)* ( $r = R_T$ ). This is the layer with optical depth  $\approx 1$  which is determined by the neutrino elastic cross section off nucleons. The cross section depends on the square of the neutrino energy, and thus  $R_T$  (as well as  $R_E$ ) is an energy-dependent quantity. Since  $R_T \gg R_{\text{res}}$  the initial asymmetry generated



at  $R_{\text{res}}$  vanishes at  $R_T$  because of multiple scatterings that completely redistribute the momentum direction of the unconverted  $\bar{\nu}_\tau$ . For  $r > R_T$  the neutrinos no longer undergo diffusion processes and freely escape from the star.

The density and temperature profile for the PNS core and atmosphere that have been used in our simulations are given by simple analytical formulae. These expressions have been chosen according to the following criteria: (i) they approximately reproduce the profiles resulting from detailed numerical studies of the PNS evolution (Burrows & Lattimer 1986); (ii) they satisfy the physical requirements that the  $\bar{\nu}_\tau$  decouple energetically with a spectral temperature  $T(R_E) \approx 8$  MeV and around densities  $\rho(R_E) \sim 10^{12}$  g cm $^{-3}$ ; (iii) they result in conservative estimates of the overall asymmetry in the sterile neutrino emission. The density profile is given by

$$\rho(r) = \begin{cases} \rho_0 \left[ 1 - \left( 1 - \frac{\rho_c}{\rho_0} \right) \left( \frac{r}{R_c} \right)^{n_c} \right] & \text{if } r \leq R_c; \\ \rho_c \left( \frac{R_c}{r} \right)^{n_a} & \text{if } r > R_c. \end{cases} \quad (7)$$

For suitable values of the exponents  $n_c$  for the core and  $n_a$  for the atmosphere, this expression reproduces reasonably well the results of a detailed numerical computation (Burrows & Lattimer 1986), namely a slowly varying density for the core ( $n_c \sim 1, 2$ ) and a steeper profile  $\sim r^{-n_a}$  (with  $n_a \sim 3-5$ ) for the atmosphere. In Fig. 2 we depict a set of profiles for different values of  $n_c$  and  $n_a$ . In our simulation we have used  $n_c = 2$ , which gives an appreciable density variation inside the core. With respect to a milder variation or to a constant profile, this is a conservative choice, since it favors the outwards diffusion of  $\bar{\nu}_\tau$  and reduces the probability of random crossings of the adiabatic resonance region. For the atmosphere we used  $n_a = 4$ , which enhances with respect to steeper profiles, the probability that some of the neutrinos will diffuse back from the atmosphere and cross the resonance region in the ‘wrong’ direction.

For the temperature profile we assumed a simple model with an isothermal core

$$T = \begin{cases} T_o & \text{if } r \leq R_c; \\ T_o \left( \frac{R_c}{r} \right)^{n_T} & \text{if } r > R_c, \end{cases} \quad (8)$$

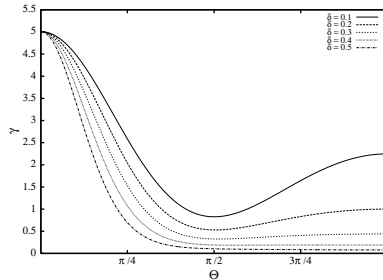


Fig. 1.— Variation of the adiabaticity parameter  $\gamma$  inside the resonance layer as a function of the angular distance  $\Theta$  from the magnetic dipole axis for different values of the decentred parameter  $\delta$ . Solid line:  $\delta = 0.1$ ; dashed:  $\delta = 0.2$ ; space-dotted:  $\delta = 0.3$ ; dotted:  $\delta = 0.4$ ; dash-dotted:  $\delta = 0.5$ . The resonance is located at  $R_{\text{res}} = 1.5 R_c$  and the maximum value of the magnetic field strength at the resonance is  $B = 4 \times 10^{15}$  G.

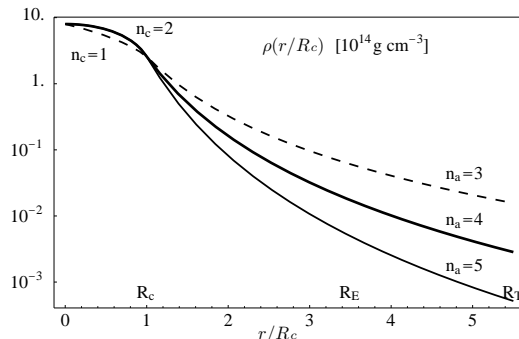


Fig. 2.— Density profiles in units of  $10^{14}$  g cm $^{-3}$  as a function of  $r/R_c$ , for different values of the exponents  $n_c$  and  $n_a$  [see Eq. (7)]. The dark solid line depicts the profile that was used in the simulations, and corresponds to  $n_c = 2$  and  $n_a = 4$ , the dashed line corresponds to  $n_c = 1$  and  $n_a = 3$ , and the light solid line corresponds to  $n_c = 2$  and  $n_a = 5$ . The position of the core–atmosphere interface ( $R_c$ ) and the approximate positions of the  $\bar{\nu}_\tau$  energy–sphere ( $R_E$ ) and transport–sphere ( $R_T$ ) are also shown.

with  $T_o = 30$  MeV (Burrows & Lattimer 1986) and  $n_T = 1$ . Since the  $\nu_s$  are emitted with spectral temperatures close to the core temperature, larger values of  $T_o$  would enhance the momentum asymmetry. During the early stage of the PNS formation, the rapid deleptonization process produces changes in the temperature on the time scale of hundreds of milliseconds. In the first few seconds after core bounce, neutrinos are emitted predominantly from the outer regions where the density is lower. Matter loses entropy, undergoes compression, and the temperature increases to values much larger than the central temperature. The temperature inversion drives the heat flux towards the interior; however, the peak temperature reaches the central regions about 10 s after core bounce, when most of the neutrinos already escaped from the core (Burrows & Lattimer 1986). Since the neutrino opacity grows with the square of the energy, a temperature inversion tends to keep the neutrinos trapped in the inner regions, enhancing the probability for their conversion. We have verified that profiles with temperature inversion generally result in larger momentum asymmetries, and thus the isothermal core represents a conservative approximation. As regards the temperature profile for the atmosphere, we assumed that it decreases with the radius as  $1/r$ . With respect to steeper temperature gradients this again favors the probability of ‘wrong’ back-crossings of the resonance.

The  $\bar{\nu}_\tau$  elastic scattering off nucleons reads

$$\frac{d\sigma_E}{d\cos\theta} = \frac{G_F^2 E_\nu^2}{8\pi} (C_1 + C_2 \cos\theta), \quad (9)$$

where  $\theta$  is the scattering angle between the incoming and outgoing neutrino directions, and the coefficients  $C_1$  and  $C_2$  depend on the neutrino–nucleon couplings averaged over the  $p$  and  $n$  number densities. For the PNS nuclear matter the canonical values  $C_A^p = -C_A^n = 1.26$  given by isospin invariance are modified due to strange-quarks contribution to the nucleon spin. We use the values  $C_V^n = -1$ ,  $C_V^p = 1 - 4\sin^2\Theta_W \simeq 0.07$ ,  $C_A^n \approx -1.15$ ,  $C_A^p \approx 1.37$  (Raffelt & Seckel 1995; Keil, Janka, & Raffelt 1995). Using also  $Y_p = 1 - Y_n \approx 0.3$  for the relative abundances of the nucleons, we obtain

$$C_1 = \sum_{N=n,p} Y_N \left[ (C_V^N)^2 + 3(C_A^N)^2 \right] \approx 5.2, \quad (10)$$

$$C_2 = \sum_{N=n,p} Y_N \left[ (C_V^N)^2 - (C_A^N)^2 \right] \approx -0.8. \quad (11)$$

Equation (9) determines the  $\bar{\nu}_\tau$  transport opacity. Inelastic reactions where the energy exchange is of order unity, such as neutrino–electron scattering and neutrino-pair processes, give only a minor contribution to the total opacity. However, they are responsible for keeping the neutrinos in thermal equilibrium with the background, and determine the relative positions of  $R_T$  and  $R_E$ . We have assumed a relative rate between inelastic and elastic processes of the order of 10%, so once every ten scatterings we generate again the neutrino energy according to the neutrino position within the star and to the corresponding local temperature. Since the  $\bar{\nu}_\tau$  emerge from the resonant layer with an overall momentum asymmetry equal and opposite to that of the  $\nu_s$ , their thermalization and especially the redistribution of their momentum due to multiple scattering is crucial for ensuring that the  $\nu_s$  momentum asymmetry is left unbalanced.

## 5. RESULTS

Neutrinos are generated randomly inside the core with a Fermi-Dirac distribution corresponding to a spectral temperature  $T_o = 30$  MeV and zero chemical potential, and are left diffusing outwards. Of course, the loss of  $\bar{\nu}_\tau$  due to conversion into sterile neutrinos eventually builds up a non-vanishing chemical potential. However, since our simulation of the neutrino diffusion is static (that is there is no time evolution of the relevant parameters characterizing the PNS model) this effect has been neglected. To study the effect of the decentred magnetic dipole, we have run simulations with  $\delta$  ranging between 0.1 and 0.6. We have also studied the effect of moving the resonance layer from inside the core ( $R_{\text{res}}/R_c = 0.8$ ,  $\rho_{\text{res}} \approx 4.5 \times \rho_{14}$ ,  $m_{\nu_s} \approx 50$  keV) to three different locations in the atmosphere  $R_{\text{res}}/R_c = 1.3, 1.5$  and 1.8 (the last value corresponds to  $\rho_{\text{res}} \approx 0.25 \times \rho_{14}$ ,  $m_{\nu_s} \approx 12$  keV). The reference value for the neutrino magnetic moment has been fixed at  $\mu_\nu = 10^{-12} \mu_B$  (of course rescaling  $\mu_\nu \rightarrow k\mu_\nu$  and  $B \rightarrow B/k$  would leave the results unchanged) and we have varied the magnetic field in the star interior between  $3 \times 10^{15}$  G and  $8 \times 10^{15}$  G. The values of  $B$  correspond to maximum values of the adiabaticity parameter at the resonance surface in the range  $\gamma \approx 3$ –12. In contrast, owing to the anisotropies of the magnetic field, in the resonance regions far from the dipole centre,  $\gamma \ll 1$ .

Once the  $\bar{\nu}_\tau$  reach the resonance, the component of the magnetic field transverse to the direction of propagation is computed, and they are converted into  $\nu_s$  with the appropriate transition probability  $P_{\bar{\nu}_\tau \leftrightarrow \nu_s}$ . The  $\nu_s$  escape from the star without interacting further. The large differences in the spatial values of  $\gamma$  can result in huge anisotropies in the conversion efficiency between different points of the resonance layer, so that the  $\nu_s$  are preferentially emitted from one hemisphere. In computing the  $\nu_s$  momentum asymmetry we have neglected the effect of gravitational redshift. On the opposite hemisphere, most of the  $\bar{\nu}_\tau$  are not converted; however, further interactions with the medium wash out their asymmetry almost completely. Of course, from regions close to the core–atmosphere interface, some  $\bar{\nu}_\tau$  can scatter inwards and resonantly convert when crossing the resonance region, so that a certain number of  $\nu_s$  will be emitted in the ‘wrong’ direction, thus reducing the overall asymmetry. When the resonance lies inside the core, this effect is somewhat enhanced since a sizeable fraction of  $\bar{\nu}_\tau$  are produced in the region  $R_{\text{res}} < r < R_c$ .

The fractional asymmetry in the total momentum of the neutrino emission needed to accelerate the remnant at a velocity  $V$  is given by

$$\frac{\Delta p}{p_{\text{tot}}} \simeq 0.03 \left( \frac{V}{10^3 \text{ km s}^{-1}} \right) \left( \frac{E_{\text{tot}}}{3 \times 10^{53} \text{ ergs}} \right) \left( \frac{M}{1.5 M_\odot} \right), \quad (12)$$

where  $E_{\text{tot}}$  is the total energy radiated in neutrinos and  $M$  is the PNS mass. Assuming equipartition of the total luminosity between the active flavours, we see that to explain velocities of several hundreds of  $\text{km s}^{-1}$  the total asymmetry in the momentum carried by the  $\nu_s$  and by the surviving  $\bar{\nu}_\tau$  ( $p(\nu_s + \bar{\nu}_\tau) \approx 0.17 p_{\text{tot}}$ ) should amount to  $\approx 10\%$ – $20\%$ . The results of different simulations run with a statistics of  $\approx 4 \times 10^5$   $\bar{\nu}_\tau$  are presented in Table I. It is apparent that momentum asymmetries of the correct size can be generated. From the table it is also possible to infer the impact that the different parameters have on the size of the asymmetry. As expected, increasing the value of the decentered parameter decreases the fractional number of  $\nu_s$  produced. The overall asymmetry first increases; however, when the conversion efficiency decreases too much, also the asymmetry gets reduced. If the resonance is inside the core, the asymmetries are generally small.

This is mainly due to the large number of ‘wrong’ crossing of the resonance region, and to some extent also to the moderate value of  $\gamma_{\text{max}}$  (larger values would require raising the magnetic field up to  $B \approx 10^{16}$  G). We stress that a crucial condition that has to be satisfied to get large asymmetries is that the adiabaticity parameter  $\gamma$  should reach values sizeably larger than unity. In fact if  $\gamma_{\text{max}} \sim 1$  the mechanism is rather inefficient, since only the  $\bar{\nu}_\tau$  with momentum almost orthogonal to the magnetic field direction will convert. Besides yielding a small conversion efficiency, this also implies that the momenta of the emerging  $\nu_s$  will be mainly oriented tangentially to the resonant layer and will not contribute to build up an asymmetry. Only for  $\gamma_{\text{max}} \gtrsim 3$ – $4$ , a sizeable momentum component in the radial direction can be generated.

If the resonance is just outside the region where most of the neutrinos are produced ( $R_{\text{res}} \gtrsim R_c$ ), asymmetries of the correct size are easily obtained. Because of the lower value of the local density, this allows for larger values of  $\gamma_{\text{max}}$  and also requires somewhat smaller magnetic fields. However, if  $\mu_\nu \lesssim 10^{-12} \mu_B$  internal magnetic field strength  $B \gtrsim 10^{15}$  G are needed in any case. Since the relevant combination that determines the value of  $\gamma$  is the product  $\mu_\nu B$ , for larger transition magnetic moments the required magnetic fields could be smaller by a factor of a few.

In spite of this, it is clear from our results that no obvious correlation between the kick velocity and the magnetic field strength can be expected. Similarly, any other correlation pattern would be quite difficult to recognize. In fact, for a given value of the neutrino transition magnetic moment  $\mu_\nu$  the efficiency of the conversion is determined by a complicated interplay between the position of the resonance layer  $R_{\text{res}}$ , the value of the decentered parameter  $\delta$ , and the strength of the magnetic field  $B$ . In some cases a large magnetic field together with a large value of  $\delta$  implies that  $\gamma \gg 1$  only in a relatively small region, thus lowering too much the conversion efficiency and implying that the  $\nu_s$  emission is mainly oriented tangentially to the resonance layer surface. Larger conversion rates are produced by smaller values of  $\delta$ , and sometimes this can also result in larger asymmetries. The exact value of the core temperature can also affect the results. For larger temperatures, about the same numbers of  $\nu_s$  will be produced, but with a

TABLE 1  
RESULTS

$\frac{R_{\text{res}}}{R_c}$	$B$	$\delta = \frac{R_B}{R_c}$	$\frac{N(\nu_s)}{N(\bar{\nu}_\tau + \nu_s)}$	$\frac{\Delta p}{p}(\nu_s)$	$\frac{\Delta p}{p}(\bar{\nu}_\tau)$	$\frac{\Delta p}{p}(\bar{\nu}_\tau + \nu_s)$
0.8	$8 \times 10^{15}$ G ( $\gamma_{\text{max}} \simeq 3.3$ )	0.1	0.58	0.03	-0.001	0.02
		0.2	0.43	0.06	-0.002	0.05
		0.3	0.27	0.09	-0.004	0.04
		0.5	0.08	0.14	-0.004	0.03
1.3	$6 \times 10^{15}$ G ( $\gamma_{\text{max}} \simeq 5.5$ )	0.2	0.57	0.11	-0.002	0.09
		0.3	0.45	0.21	-0.010	0.15
		0.4	0.33	0.29	-0.006	0.17
		0.6	0.17	0.44	-0.004	0.17
1.5	$6 \times 10^{15}$ G ( $\gamma_{\text{max}} \simeq 11.3$ )	0.3	0.51	0.13	+0.003	0.10
		0.4	0.48	0.21	-0.005	0.16
		0.5	0.44	0.27	-0.002	0.16
		0.6	0.29	0.37	-0.002	0.21
1.5	$4 \times 10^{15}$ G ( $\gamma_{\text{max}} \simeq 5.0$ )	0.2	0.54	0.11	-0.005	0.09
		0.3	0.44	0.19	+0.001	0.12
		0.4	0.37	0.26	-0.006	0.17
		0.5	0.26	0.36	-0.003	0.15
1.8	$3 \times 10^{15}$ G ( $\gamma_{\text{max}} \simeq 7.0$ )	0.2	0.60	0.09	-0.011	0.07
		0.3	0.58	0.12	+0.006	0.09
		0.4	0.43	0.22	+0.003	0.15
		0.6	0.28	0.39	+0.006	0.10

NOTE.—The results of our simulations. Different positions of the resonance layer have been studied: inside the core ( $R_{\text{res}}/R_c = 0.8$ ) and outside the core ( $R_{\text{res}}/R_c = 1.3, 1.5, 1.8$ ). The values of the magnetic field are given in the second column, together with the corresponding maximum value of the adiabaticity parameter  $\gamma$ . In all the simulations we have assumed  $\mu_\nu = 10^{-12} \mu_B$ . The displacement of the magnetic dipole from the star centre  $\delta = R_B/R_c$  is listed in the third column, while the resulting overall efficiency for  $\bar{\nu}_\tau$  conversion into  $\nu_s$  is given in the fourth column. The momentum asymmetry for the  $\nu_s$ , for the unconverted  $\bar{\nu}_\tau$ , and the overall  $\bar{\nu}_\tau + \nu_s$  momentum asymmetry are given in the last three columns respectively.

higher spectral temperature. This effect tends to increase the asymmetry.

Finally, we should mention that since the  $\nu_s$  emission is likely to occur on a time scale much larger than the pulsar rotational period at birth, the resulting momentum kick would be averaged out proportionally to the cosine of the angle between the spin axis and the magnetic axis. However, even if we assume that the present orientation of the magnetic axis is representative of its orientation at birth, we believe that it is not possible to predict any unambiguous correlation between the pulsars' velocities and their magnetic axis orientation, because of the large number of different parameters that concur to determine the overall effect.

In conclusion, we have shown that  $\bar{\nu}_\tau \leftrightarrow \nu_s$  RSFP inside the PNS core is able to account for pulsar natal kicks of the required size. The crucial assumptions to achieve this result are (i) the presence of sizeable anisotropies in the PNS magnetic field configuration; (ii) internal magnetic field strengths of the order of few  $\times 10^{15}$  G; (iii) a sterile neutrino with a mass of a few tens of keV and with a transition magnetic moment with an active flavour of the order of  $10^{-12} \mu_B$ . The first two assumptions have already been discussed in this paper, so let us comment briefly on the last point. If all the active neutrinos have a mass satisfying the cosmological limit  $\lesssim 100$  eV, it would be somewhat complicated to construct a particle physics model that realizes the third condition, since a large magnetic moment generally implies rather large radiative contributions to the neutrino masses. This problem was extensively addressed in the past, and some clever solutions were proposed (Voloshin 1988; Barbieri & Mohapatra 1989). We believe that a consistent particle physics model yielding a large  $\bar{\nu}_\tau - \nu_s$  transition magnetic moment and a light  $\nu_\tau$  can be constructed along the same lines. Let us also mention that quite recently the cosmological limits on neutrino masses have been revisited under the hypothesis that the Universe underwent a non-trivial thermal evolution right before the nucleosynthesis era (Giudice, Kolb & Riotto 2000). The result of this study opens up the possibility that also  $m_{\nu_\tau}$  could be of the order of a few tens of keV. Indeed this would render the whole picture much more natural from the particle physics point of view.

This work was supported in part by BID and Colciencias in Colombia under contract 401-97 code 1115-05-087-97. We acknowledge E. Akhmedov for useful conversations and M. Kachelriess for bringing to our attention the work of Oberauer et al. (1993).

## REFERENCES

- Akhmedov, E. K. 1988a, *Sov. J. Nucl. Phys.* 48, 382; 1988b, *Phys. Lett.* B213, 64
- Akhmedov, E. K. 1997, preprint (astro-ph/9705451)
- Akhmedov, E. K., Lanza, A., & Sciama, D. W. 1997, *Phys. Rev.* D56, 6117
- Arras, P., & Lai, D. 1999, *Phys. Rev.* D60, 043001
- Ayala, A., D'Olivo, J. C., & Torres, M. 2000, *Nucl. Phys.* B564, 204
- Barbieri, R., & Mohapatra, R. N. 1988, *Phys. Rev. Lett.* 61, 27
- Barbieri, R., & Mohapatra, R. N. 1989, *Phys. Lett.* B218, 225
- Bergmann, S., Grossman, Y., & Nardi, E. 1999, *Phys. Rev.* D60, 093008
- Botella, F. J., Lim, C. S., & Marciano, W. J. 1987, *Phys. Rev.* D35, 896
- Burrows, A., & Hayes, J. 1995, preprint (astro-ph/9506057)
- Burrows, A., & Hayes, J. 1996, *Phys. Rev. Lett.* 76, 352
- Burrows, A., & Lattimer, J. M. 1986, *ApJ* 307, 178
- Cordes, J. M., & Chernoff, D. F. 1997, preprint (astro-ph/9707308)
- Cowsik, R. 1998, *A&A* 340, 65
- Deshpande, A. A., Ramachandran, R., & Radhakrishnan, V. 1999, *A&A* 351, 195
- Dewey, R. J., & Cordes, J. M. 1987, *ApJ* 321, 780
- Elmfors, P., Enqvist, K., Raffelt, G., & Sigl, G. 1997, *Nucl. Phys.* B503, 3

- Giudice, G. F., Kolb, E. W., & Riotto, A. 2000, preprint hep-ph/0005123
- Gott, J. R., Gunn, J. E., & Ostriker, J. P. 1970, ApJ 160, L91
- Grasso, D., Nunokawa, H., & Valle, J. W. 1998, Phys. Rev. Lett. 81, 2412
- Groom, D., E. et al. 1998, Eur. Phys. J. C3, 1
- Gunn, L. E., & Ostriker, J. P. 1970, ApJ 160, 979
- Hankins, T. H., & Fowler, L. A. 1986, ApJ 304, 256
- Hannestad, S., Janka, H. T., Raffelt, G. G., & Sigl, G. 1999, preprint (astro-ph/9912242)
- Hansen, B. M. S., & Phinney, B. M. S. 1997, MNRAS 291, 569
- Harrison, E. R., & Tademaru, E. 1975, ApJ 201, 447
- Horowitz, C. J., & Li, G. 1998, Phys. Rev. Lett. 80, 3694
- Horowitz, C. J., & Piekarewicz, J. 1998, Nucl. Phys. A640, 281
- Hughes, A., & Bailes, M. 1999, ApJ 522, 504
- Hurley, K. 1999, preprint (astro-ph/9912061)
- Iben, I., & Tutukov, A. 1996, ApJ 456, 738; 1997, ApJ 491, 303
- Janka, H. T. 1995, Astropart. Phys. 3, 377
- Janka, H. T., & Mueller, E. 1994, A&A 290, 496
- Janka, H. T., & Raffelt, G. G. 1999, Phys. Rev. D59, 023005
- Keil, W., Janka, H. T., & Raffelt, G. 1995, Phys. Rev. D51, 6635
- Kusenko, A. & Segrè, G. 1996, Phys. Rev. Lett. 77, 4872; 1997, Phys. Lett. B396, 197
- Kusenko, A., Segrè, G., & Vilenkin, A. 1998, Phys. Lett. B437, 359
- Lai, D. 1999, preprint (astro-ph/9912522)
- Lai, D., & Qian, Y. 1998a, ApJ 495, L103
- Lai, D., & Qian, Y. 1998b, ApJ 505, 884
- Landstreet, J. D. 1970, ApJ 159, 1001
- Lim, C., & Marciano, W. J. 1988, Phys. Rev. D37, 1368
- Lorimer, D. R., Bailes, M., & Harrison, P. A. 1997, MNRAS 289, 592
- Lyne, A. G., & Lorimer, D. R. 1994, Nature 369, 127
- Mikhhev, S. P., & Smirnov, A. Y. 1985, Sov. J. Nucl. Phys. 42, 913
- Nunokawa, H., Semikoz, V. B., Smirnov, A. Y., & Valle, J. W. 1997, Nucl. Phys. B501, 17
- Oberauer, L., Hagner, C., Raffelt, G., & Rieger, E. 1993, Astropart. Phys. 1, 377
- Ostriker, J. P., & Gunn, J. E. 1969, ApJ 157, 1395
- Raffelt, G. G. 1990, Phys. Rev. Lett. 64, 2856; 1999, Phys. Rep. 320, 319
- Raffelt, G. 1996, Stars as laboratories for fundamental Physics, (The University of Chicago Press)
- Raffelt, G., & Seckel, D. 1995, Phys. Rev. D52, 1780
- Raffelt, G., & Sigl, G. 1993, Astropart. Phys. 1, 165
- Spruit, H. C., & Phinney, E. S. 1998, Nature 393, 139
- Tademaru, E. & Harrison, E. R. 1975, Nature 254, 676
- Tademaru, E. 1976, ApJ 209, 245
- Thompson, C. & Duncan, R. C. 1992, ApJ 392, L9; 1993, ApJ 408, 194; 1995, MNRAS 275, 255; 1996, ApJ 473, 322
- van den Heuvel, E. P. J., & van Paradijs, J. 1997, ApJ 483, 399
- Voloshin, M. B. 1988, Sov. J. Nucl. Phys. 48, 512
- Wolfenstein, L. 1978, Phys. Rev. D17, 2369

This 2-column preprint was prepared with the AAS L<sup>A</sup>T<sub>E</sub>X macros v5.0.